

WL-TR-97-4009

EFFECTS ON STRESS SINGULARITIES OF
INTRODUCING COHESIVE STRESS-SEPARATION LAWS
AS BOUNDARY CONDITIONS FOR ELASTIC PLATES IN
EXTENSION



GLENN B. SINCLAIR, PH.D.

SYSTRAN CORPORATION
4126 LINDEN AVENUE
DAYTON, OH 45432-3068

DECEMBER 1995

INTERIM REPORT FOR 08/01/95-09/29/95

APPROVED FOR PUBLIC RELEASE; DISTRIBUTION IS UNLIMITED.

DTIC QUALITY INSPECTED 2

19970423 026

MATERIALS DIRECTORATE
WRIGHT LABORATORY
AIR FORCE MATERIEL COMMAND
WRIGHT PATTERSON AFB OH 45433-7734

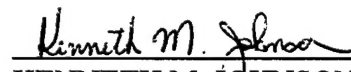
NOTICE

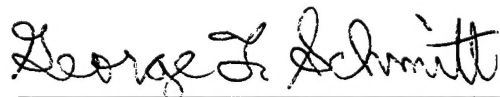
WHEN GOVERNMENT DRAWINGS, SPECIFICATIONS, OR OTHER DATA ARE USED FOR ANY PURPOSE OTHER THAN IN CONNECTION WITH A DEFINITE GOVERNMENT-RELATED PROCUREMENT, THE UNITED STATES GOVERNMENT INCURS NO RESPONSIBILITY OR ANY OBLIGATION WHATSOEVER. THE FACT THAT THE GOVERNMENT MAY HAVE FORMULATED OR IN ANY WAY SUPPLIED THE SAID DRAWINGS, SPECIFICATIONS, OR OTHER DATA, IS NOT TO BE REGARDED BY IMPLICATION, OR OTHERWISE IN ANY MANNER CONSTRUED, AS LICENSING THE HOLDER, OR ANY OTHER PERSON OR CORPORATION; OR AS CONVEYING ANY RIGHTS OR PERMISSION TO MANUFACTURE, USE, OR SELL ANY PATENTED INVENTION THAT MAY IN ANY WAY BE RELATED THERETO.

THIS REPORT IS RELEASABLE TO THE NATIONAL TECHNICAL INFORMATION SERVICE (NTIS). AT NTIS, IT WILL BE AVAILABLE TO THE GENERAL PUBLIC, INCLUDING FOREIGN NATIONS.

THIS TECHNICAL REPORT HAS BEEN REVIEWED AND IS APPROVED FOR PUBLICATION.


MAYRA I. MARTINEZ
Program Manager


KENNETH M. JOHNSON
Materials Engineer


GEORGE F. SCHMITT, Chief
Integration and Operations Division
Materials Directorate

IF YOUR ADDRESS HAS CHANGED, IF YOU WISH TO BE REMOVED FROM OUR MAILING LIST, OR IF THE ADDRESSEE IS NO LONGER EMPLOYED BY YOUR ORGANIZATION, PLEASE NOTIFY WL/MLI, WRIGHT-PATTERSON AFB OH 45433-7746 TO HELP MAINTAIN A CURRENT MAILING LIST.

Copies of this report should not be returned unless return is required by security considerations, contractual obligations, or notice on a specific document.

REPORT DOCUMENTATION PAGE			Form Approved OMB No. 0704-0188	
Public reporting burden for this collection of information is estimated to average 1 hour per response, including the time for reviewing instructions, searching existing data sources, gathering and maintaining the data needed, and completing and reviewing the collection of information. Send comments regarding this burden estimate or any other aspect of this collection of information, including suggestions for reducing this burden, to Washington Headquarters Services, Directorate for Information Operations and Reports, 1215 Jefferson Davis Highway, Suite 1204, Arlington, VA 22202-4302, and to the Office of Management and Budget, Paperwork Reduction Project (0704-0188), Washington, DC 20503.				
1. AGENCY USE ONLY (Leave blank)	2. REPORT DATE December 1995	3. REPORT TYPE AND DATES COVERED Interim Report 1 Aug 1995-29 Sep 1995		
4. TITLE AND SUBTITLE The Effects on Stress Singularities of Introducing Cohesive Stress-Separation Laws as Boundary Conditions for Elastic Plates in Extension		5. FUNDING NUMBERS C: F33615-94-C-5804 PE: 62102F PR: 2418 TA: 00 WU: VS		
6. AUTHOR(S) Glenn B. Sinclair, Ph.D.				
7. PERFORMING ORGANIZATION NAME(S) AND ADDRESS(ES) SYSTRAN Corporation 4126 Linden Avenue Dayton, OH 45432-3068		8. PERFORMING ORGANIZATION REPORT NUMBER		
9. SPONSORING/MONITORING AGENCY NAME(S) AND ADDRESS(ES) Materials Directorate Wright Laboratory Wright-Patterson AFB, OH 45433 POC: Mayra I. Martinez, WL/MLI (937) 255-7174		10. SPONSORING/MONITORING AGENCY REPORT NUMBER WL-TR-97-4009		
11. SUPPLEMENTARY NOTES				
12a. DISTRIBUTION/AVAILABILITY STATEMENT Approved for public release; distribution is unlimited.		12b. DISTRIBUTION CODE		
13. ABSTRACT (Maximum 200 words) The nature of the stress field occurring at the vertex of an angular elastic plate in extension is reconsidered. An additional boundary condition is introduced. This boundary condition reflects the action of cohesive stress-separation laws. Companion asymptotic analysis follows the well-known approach of introducing separable forms for the Airy stress function in polar coordinates, then solving the associated eigenvalue problem. Now, though, eigenfunctions typically occur as power series in the radial coordinate, rather than as closed form functions of this variable. The end result of the analysis is a reduction in the number of angular plate configurations which can promote singular stresses. This elimination of singular behavior is demonstrated for a crack and a sharp reentrant corner under transverse tension, and for an epoxy-steel butt joint and a three phase junction in a titanium aluminide microstructure. All of these examples have singular stress fields when treated with classical boundary conditions: none of them do when appropriate cohesive stress-separation laws are introduced.				
14. SUBJECT TERMS Elastic Stress Singularities Cohesive Stress-Separation Elastic Plate Stress Fields			15. NUMBER OF PAGES 47	
			16. PRICE CODE	
17. SECURITY CLASSIFICATION OF REPORT Unclassified	18. SECURITY CLASSIFICATION OF THIS PAGE Unclassified	19. SECURITY CLASSIFICATION OF ABSTRACT Unclassified	20. LIMITATION OF ABSTRACT SAR	

THE EFFECTS ON STRESS SINGULARITIES OF INTRODUCING COHESIVE STRESS-SEPARATION LAWS AS BOUNDARY CONDITIONS FOR ELASTIC PLATES IN EXTENSION

Table of Contents

Abstract	iii
List of figures and tables	vi
Preface	v
Introduction	1
1. Formulation	6
2. Equivalent boundary conditions for cohesive stress-separation laws	10
3. Eigenvalue equations	16
4. Eigenfunctions for some special cases	21
Concluding remarks	36
References	38
Appendix	39

THE EFFECTS ON STRESS SINGULARITIES OF INTRODUCING COHESIVE STRESS-SEPARATION LAWS AS BOUNDARY CONDITIONS FOR ELASTIC PLATES IN EXTENSION

List of figures

- Fig. 1. Crack with local cohesive zone (after Barenblatt [4]) - p. 2
- Fig. 2. Close up of crack tip with cohesive stresses both ahead and in back of the tip (the original tip O takes up two positions, O^+ and O^-) - p. 5
- Fig. 3. Angular elastic plate and coordinates - p. 7
- Fig. 4. Schematic of a normal cohesive stress-separation law - p. 11
- Fig. 5. Singularity exponents for cohesive stress boundary conditions - p. 19
- Fig. 6. Some special cases: (a) crack tip, (b) reentrant corner, (c) epoxy-steel butt joint and (d) junction of phases in TiAl microstructure - p. 22

List of tables

- Table 1. Homogeneous boundary conditions for plate edges - p. 8
- Table 2. Eigenvalue equations with cohesive stress boundary conditions - p. 18

THE EFFECTS ON STRESS SINGULARITIES OF INTRODUCING COHESIVE STRESS-SEPARATION LAWS AS BOUNDARY CONDITIONS FOR ELASTIC PLATES IN EXTENSION

Preface

This research project was conducted under Air Force Contract F33615-94-C-5804, "Contributive Research and Development," Task 36, sponsored by Wright Laboratory, Materials Directorate, Materials Behavior Branch (MLLN) at Wright-Patterson AFB, Ohio. The Air Force Program Manager was Ms. Angela Annaballi. The Air Force Technical Manager was Dr. James M. Larsen. The Principal Investigator was Dr. Glenn B. Sinclair. The SYSTRAN Corporation Program Manager was Mr. M.E. Zellmer.

THE EFFECTS ON STRESS SINGULARITIES OF INTRODUCING COHESIVE STRESS-SEPARATION LAWS AS BOUNDARY CONDITIONS FOR ELASTIC PLATES IN EXTENSION

Abstract

The nature of the stress field occurring at the vertex of an angular elastic plate in extension is reconsidered. An additional boundary condition is introduced. This boundary condition reflects the action of cohesive stress-separation laws. Companion asymptotic analysis follows the well-known approach of introducing separable forms for the Airy stress function in polar coordinates, then solving the associated eigenvalue problem. Now, though, eigenfunctions typically occur as power series in the radial coordinate, rather than as closed form functions of this variable. The end result of the analysis is a reduction in the number of angular plate configurations which can promote singular stresses. This elimination of singular behavior is demonstrated for a crack and a sharp reentrant corner under transverse tension, and for an epoxy-steel butt joint and a three phase junction in a titanium aluminide microstructure. All of these examples have singular stress fields when treated with classical boundary conditions: none of them do when appropriate cohesive stress-separation laws are introduced.

THE EFFECTS ON STRESS SINGULARITIES OF INTRODUCING COHESIVE STRESS-SEPARATION LAWS AS BOUNDARY CONDITIONS FOR ELASTIC PLATES IN EXTENSION

Introduction

The stress fields in angular elastic plates in extension were first treated by Knein [1], and subsequently systematically identified by Williams [2]. These studies reveal the possibility of elastic *stress singularities* at the vertex of the wedge. For example, a stress-free wedge of angle 2π realizes a model of a crack having stresses which behave as the inverse of the square root of the distance from the crack tip. Such fields are at variance with the assumptions underlying the theory from which they came. Consequently, care needs to be exercised in interpreting them. Even with care, resulting inferences with respect to structural integrity are not always as reliable as desired in practice (see, for example, [3]). Accordingly it is of some interest to explore alternative models which are free of these nonphysical singular stresses. This report considers a means to this end, namely the introduction of cohesive stress-separation laws.

Barenblatt was first to introduce *cohesive stress-separation laws* to rid cracks of their stress singularities; an extensive account of his work is given in [4]. Essentially his approach *cancels* the opening singularity produced by loading remote from the crack with the closing singularity produced by cohesive stresses on the crack flanks near the crack tip.

To explain further, we consider the example of a central crack in an infinite elastic plate under far-field uniform tension (Fig. 1). The crack has length $2a$, the applied tension magnitude σ_0 . To describe the configuration, we use rectangular Cartesian coordinates x, y , with origin O at the rightmost crack tip. Then the normal definition of the *stress intensity factor*, K_I , associated with this crack tip, has

$$K_I = \lim_{x \rightarrow 0^+} \sqrt{2\pi x} \left. \sigma_y \right|_{y=0}, \quad (1)$$

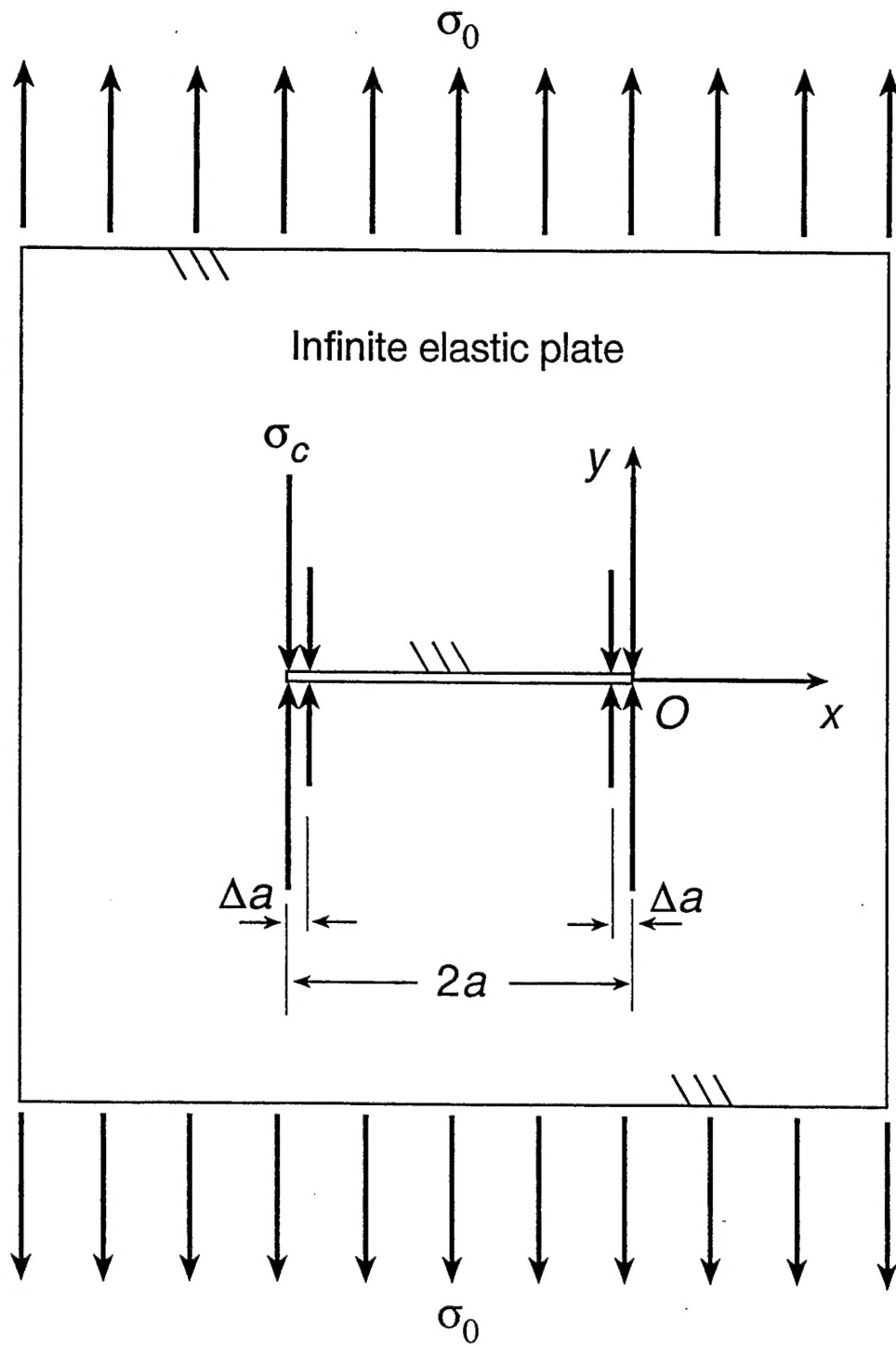


Fig. 1. Crack with local cohesive zone (after Barenblatt [4])

where σ_y is the normal stress component in the y-direction. Accordingly, K_I is the coefficient of the aforementioned inverse-square-root singularity in the crack-tip stress field. Its values for the central crack configuration of Fig. 1 are as follows. For the applied stress σ_0 , we have (see, e.g., Tada, Paris and Irwin [5], p. 5.1)

$$K_I = \sigma_0 \sqrt{\pi a}. \quad (2)$$

For the cohesive stress, $\sigma_c = \sigma_c(\xi)$ where $\xi = -x$, we have (see, e.g., Tada et al., [5], p. 5.11)

$$K_I = -\sqrt{\frac{a}{\pi}} \int_0^{\Delta a} \frac{2\sigma_c(\xi)d\xi}{\sqrt{\xi(2a-\xi)}}, \quad (3)$$

where Δa is the extent of the zones in which the cohesive stresses act. Thus by ensuring the magnitudes of the stress intensity factors in (2), (3) are equal, the advertised cancellation takes place and effects a singularity-free crack.

In addition to introducing cohesive stresses, Barenblatt made some assumptions regarding their distribution. First, he assumes that the extent of the cohesive zones is small ([4], p. 78), i.e., $\Delta a / a \ll 1$. Under this assumption, the stress intensity factor of (3) is given by

$$K_I = -\sqrt{\frac{2}{\pi}} K \left[1 + O\left(\frac{\Delta a}{a}\right) \right], \quad (4)$$

$$K = \int_0^{\Delta a} \frac{\sigma_c(\xi)}{\sqrt{\xi}} d\xi,$$

as $\Delta a / a \rightarrow 0$, wherein O is the large order O symbol. Barenblatt terms K of (4) the *modulus of cohesion*. His second assumption then has, in effect, that the maximum possible value of K does not depend upon the applied loading, σ_0 , and is always the same for a given material ([4], p. 79). Thus when this maximum is attained and fracture is about to occur, provided the configuration is maintained singularity free, the stress intensity factor due to σ_0 has also attained a critical value. Essentially, then, the stress intensity factor due to applied loading becomes the key parameter controlling fracture, the *same fracture criterion* as used in fracture mechanics when *singularities are present*. Goodier [6] and Rice [7] also provide arguments that, as a result of his assumptions, Barenblatt's approach reduces to the same as for cracks with singularities present. Hence, while Barenblatt does indeed cancel singularities for cracks by introducing the concept of cohesive crack-flank stresses, the manner in which he does so leads to an approach which is equivalent to that used when singularities are present as far as fracture goes. As a consequence, this cancellation of singular behavior is perhaps not that significant from a practical viewpoint.

Here, in contrast, we do not assume the cohesive zone to be necessarily small. In fact, we let it extend ahead of the crack tip, as indicated in the sketch of Fig. 2. This extension changes the boundary conditions ahead of the crack. Since boundary conditions play a critical role in determining the possible singular behavior present, this change raises the question, "what type of singularity can the crack now have?" We seek to investigate this question herein, both for the cracked plate in particular, and for the angular plate in general.

We begin in Section 1 with a formal problem statement. Next, in Section 2, we develop boundary conditions equivalent to cohesive stress-separation laws which, in turn, lead to the eigenvalue equations given in Section 3. We then examine some associated eigenfunctions for special cases in Section 4, and close by offering some concluding remarks.

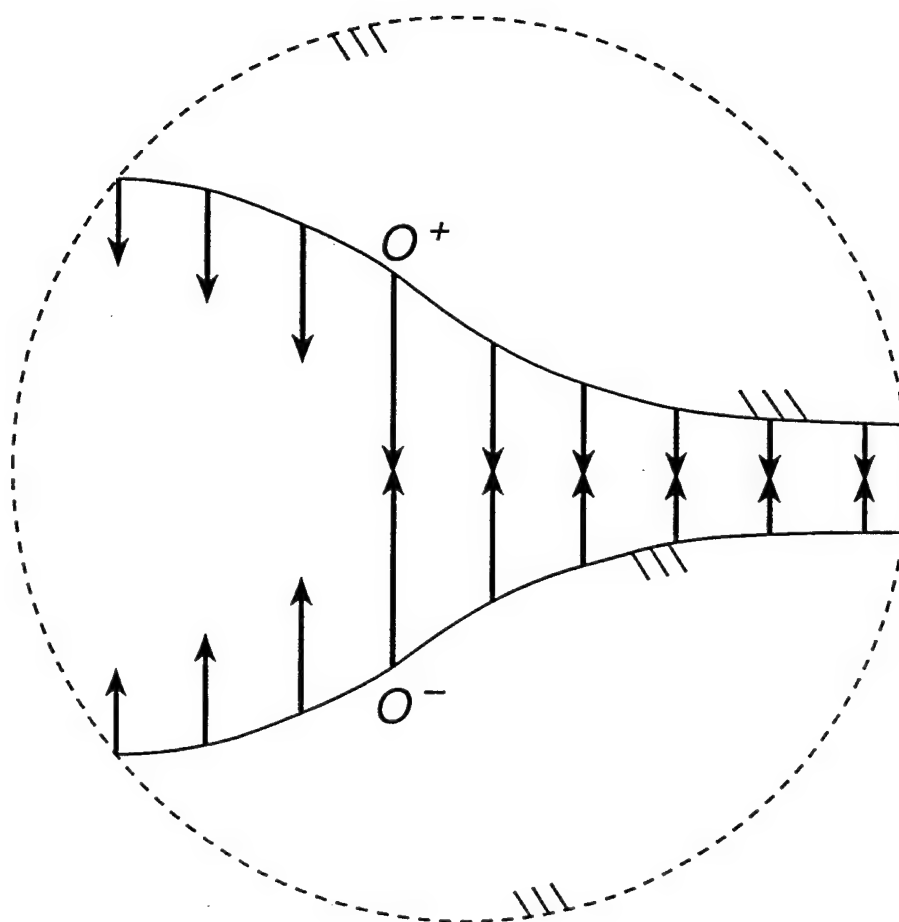


Fig. 2. Close up of crack tip with cohesive stresses both ahead and in back of the tip (the original tip O takes up two positions, O^+ and O^-)

1. Formulation

Here we specify, in some detail, the class of angular elastic plate configurations to be examined for possible stress singularities.

To facilitate the treatment of the angular plate geometry (Fig. 3), we use polar coordinates r, θ , sharing the same origin, O , as their rectangular counterparts x, y , and related to them as in:

$$x = r \cos \theta, \quad y = r \sin \theta, \quad (5)$$

for $0 < r < \infty$, $0 \leq \theta < 2\pi$. Then the region of interest, \mathfrak{R} , is given by:

$$\mathfrak{R} = \{(r, \theta) | 0 < r < \infty, \quad 0 < \theta < \phi\}, \quad (6)$$

where ϕ is the vertex angle of the angular plate. With these geometric preliminaries in place, we can formulate the class of problems of concern as follows.

In general, we seek the two-dimensional, elastic, stress components $\sigma_r, \sigma_\theta, \tau_{r\theta}$, and associated displacements u_r, u_θ , satisfying the following: the *stress equations of equilibrium* in the absence of body forces,

$$\begin{aligned} \frac{\partial \sigma_r}{\partial r} + \frac{1}{r} \frac{\partial \tau_{r\theta}}{\partial \theta} + \frac{\sigma_r - \sigma_\theta}{r} &= 0, \\ \frac{1}{r} \frac{\partial \sigma_\theta}{\partial \theta} + \frac{\partial \tau_{r\theta}}{\partial r} + \frac{2\tau_{r\theta}}{r} &= 0, \end{aligned} \quad (7)$$

on \mathfrak{R} ; the *stress-displacement relations* for a homogeneous and isotropic, linear elastic plate, in a state of plane strain,

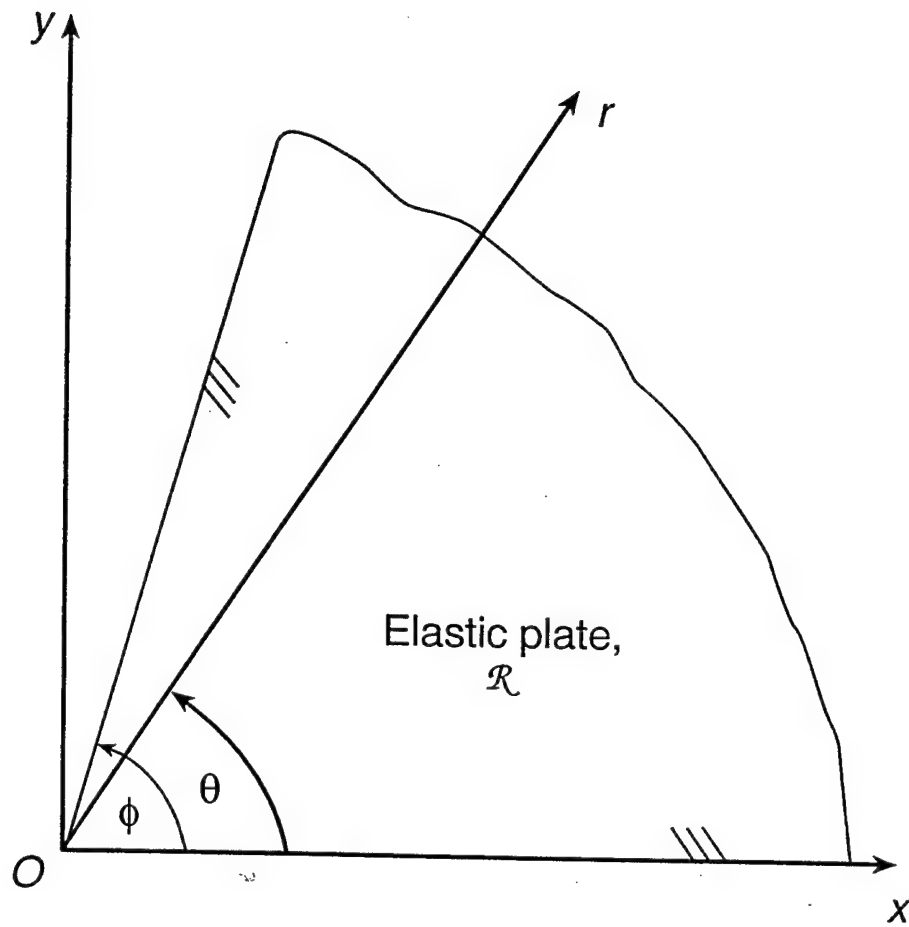


Fig. 3. Angular elastic plate and coordinates

$$\begin{aligned}
\sigma_r &= \frac{2\mu}{1-2\nu} \left[(1-\nu) \frac{\partial u_r}{\partial r} + \nu \left(\frac{1}{r} \frac{\partial u_\theta}{\partial \theta} + \frac{u_r}{r} \right) \right], \\
\sigma_\theta &= \frac{2\mu}{1-2\nu} \left[(1-\nu) \left(\frac{1}{r} \frac{\partial u_\theta}{\partial \theta} + \frac{u_r}{r} \right) + \nu \frac{\partial u_r}{\partial r} \right], \\
\tau_{r\theta} &= \mu \left[\frac{1}{r} \frac{\partial u_r}{\partial \theta} + \frac{\partial u_\theta}{\partial r} - \frac{u_\theta}{r} \right],
\end{aligned} \tag{8}$$

on \mathfrak{R} , for $0 < r < \infty$, wherein μ is the shear modulus, ν Poisson's ratio[†]; and *cohesive stress boundary conditions* on $\theta = 0$ together with any of the admissible set of boundary conditions given in Table 1 on $\theta = \phi$ for $0 < r < \infty$. Specifically, we are interested in the local behavior of the fields complying with the foregoing in the vicinity of the wedge vertex, O.

Table 1. Homogeneous boundary conditions for plate edges

No.	Conditions	Description
(i)	$\sigma_\theta = k u_\theta, \quad \tau_{r\theta} = k' u_r$	Cohesive stress-separation laws
(ii)	$\sigma_\theta = 0, \quad \tau_{r\theta} = 0$	Stress free
(iii)	$u_r = 0, \quad u_\theta = 0$	Clamped/rigid adhesive contact
(iv)	$u_\theta = 0, \quad \tau_{r\theta} = 0$	Symmetry/rigid lubricated contact
(v)	$u_r = 0, \quad \sigma_\theta = 0$	Antisymmetry

[†] For plane stress, replace ν by $\nu / (1 + \nu)$.

Several comments are appropriate at this point. We begin this commentary by considering the general nature of the preceding formulation, then focus the discussion on each of the boundary conditions in Table 1 in turn.

First with respect to the selection of plane strain (or plane stress) field equations, we remark that results found can be expected to apply to axisymmetric configurations, and even three-dimensional ones provided the geometry varies smoothly enough in the out-of-plane direction (Aksentian [8]). Second re the choice of homogeneous boundary conditions, we observe that typically singular behavior is controlled by these conditions rather than their inhomogeneous counterparts.[†] Third regarding the absence of regularity requirements at infinity on the open wedge \mathcal{R} , we note that this renders fields complying with our formulation nonunique. Since the principal attribute of these fields is the potential characterization of all possible responses at the wedge vertex, such a lack of uniqueness is to be desired rather than regulated against.

Turning to the specific boundary conditions in Table 1, the first set is that associated with cohesive stresses. Thus k, k' in (i) are stiffnesses associated with *relative* displacements between material on the two sides of the ray on which the condition is applied. These "springs" need not be linear; in fact, typically $k = k(u_\theta)$, $k' = k'(u_r)$. The second and third conditions are the traditional "free" and "clamped" cases treated by Williams [2]; the latter of these two also admits to interpretation as the homogeneous complement to indentation by a rigid punch with complete adhesion. These three sets of boundary conditions realize three problems within the class under consideration: (i) - (i), (i) - (ii), and (i) - (iii). In the instance wherein the cohesive stress conditions are taken on both faces, it is useful to distinguish between symmetric and antisymmetric response. The next two sets of boundary conditions, (iv) and (v), enable one to do this. The symmetry conditions can also be interpreted as the homogeneous complement to

[†] Usually there are no singularities which stem from the inhomogeneous part of physically sensible boundary conditions. However, jump discontinuities from one wedge face to the other in $\tau_{r\theta}$ or u_θ / r can produce $\ln r$ stress singularities.

indentation by a perfectly smooth, or lubricated, rigid punch. In all, therefore, the independent problems within the class of present concern are: (i) - (ii), (i) - (iii), (i) - (iv), and (i) - (v).

2. Equivalent boundary conditions for cohesive stress-separation laws

In this section, we consider the role of cohesive stress-separation laws as boundary conditions to see the degree to which it can be reduced to that of other, more traditional, boundary conditions. In this way we hope to reduce the analysis of cohesive stress boundary conditions by taking advantage of known asymptotic solutions.

A sketch of a normal cohesive stress versus separation law stemming from attraction/repulsion between atoms/molecules is shown in Fig. 4. Therein s is the separation, s_e its equilibrium value. As the slope varies, we can expect k of (i), Table 1, to be a function of separation. However, initially as loading commences, a constant stiffness is a fair approximation (as indicated by the dashed line in Fig. 4). Thus we take k to be constant henceforth. For similar reasons, we can also approximate k' as being constant.

To simplify matters further, we temporarily take $k' = 0$ and focus on the normal cohesive stress. That is, we consider

$$\sigma_\theta = k u_\theta, \quad \tau_{r\theta} = 0 \quad \text{at} \quad \theta = 0, \quad (9)$$

for $0 < r < \infty$, where k is now constant. This simplification is actually an appropriate one if cohesive stresses act on a line of symmetry, because then there is no relative u_r and $\tau_{r\theta} = 0$. Notice, too, that on such a line u_θ need not be zero if cohesive stresses act (e.g., Fig. 2), in contrast to the symmetry conditions in (iv), Table 1.

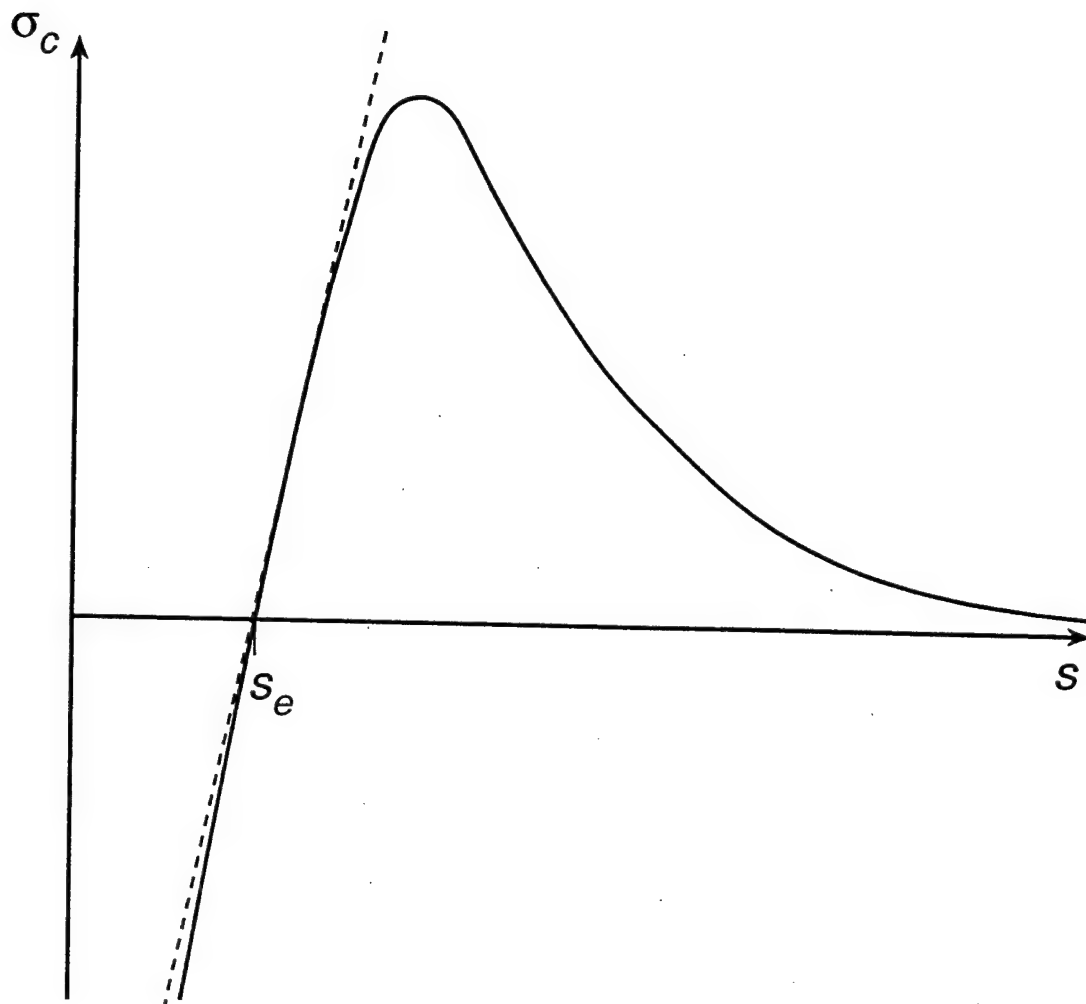


Fig. 4. Schematic of a normal cohesive stress-separation law

Prior to actually complying with (9), we need to construct stress and displacement fields satisfying the governing equations, (7), (8). Following Knein [1], Williams [2], we use the Airy stress function, χ , to this end. That is, we take

$$\begin{aligned}\sigma_r &= \frac{1}{r^2} \frac{\partial^2 \chi}{\partial \theta^2} + \frac{1}{r} \frac{\partial \chi}{\partial r}, \\ \sigma_\theta &= \frac{\partial^2 \chi}{\partial r^2}, \\ \tau_{r\theta} &= -\frac{\partial}{\partial r} \left(\frac{1}{r} \frac{\partial \chi}{\partial \theta} \right),\end{aligned}\tag{10}$$

throughout \mathfrak{R} , with

$$\nabla^4 \chi = 0,\tag{11}$$

on \mathfrak{R} , ∇^4 being the biharmonic operator. While χ is biharmonic, it can be obtained as a combination of harmonic functions, ψ_1 and ψ_2 , via

$$\chi = \psi_1 + r^2 \psi_2.\tag{12}$$

The key in choosing ψ_1 and ψ_2 is to ensure that the resulting χ has four linearly independent functions of θ which share a common r -dependence: then when boundary conditions are ultimately applied on $\theta = 0, \phi$, we will have available four arbitrary coefficients, or constants, to satisfy the four conditions involved. With this in mind, we start by selecting the classical separable solution for ψ_1 ,

$$\psi_1 = r^{\lambda+1} [A \cos(\lambda+1)\theta + B \sin(\lambda+1)\theta].\tag{13}$$

In (13), A and B are two of the required constants, and the exponent $\lambda+1$ is chosen merely for subsequent convenience in expressing eigenvalue equations (after Williams [2]). Next, to obtain two more functions of θ which share $r^{\lambda+1}$ as a coefficient, we exchange $\lambda+1$ for $\lambda-1$ in (13) and take

$$\psi_2 = r^{\lambda-1} [C \cos(\lambda-1)\theta + D \sin(\lambda-1)\theta], \quad (14)$$

where C and D are two further constants. Combining ψ_1 and ψ_2 in accordance with (12) then yields the desired χ with a total of four constants with the same $r^{\lambda+1}$ multiplier. The attendant stresses can be derived directly from the Airy stress function relations (10). The corresponding displacements can be similarly determined with the aid of a further auxiliary harmonic function (see Williams [2] for details), or simply by integrating the stress-displacement relations (8). The resulting fields have, for the stresses,

$$\begin{aligned} \sigma_r &= -\lambda r^{\lambda-1} [(\lambda-3)(a \cos(\lambda-1)\theta + b \sin(\lambda-1)\theta) + c \cos(\lambda+1)\theta + d \sin(\lambda+1)\theta], \\ \sigma_\theta &= \lambda r^{\lambda-1} [(\lambda+1)(a \cos(\lambda-1)\theta + b \sin(\lambda-1)\theta) + c \cos(\lambda+1)\theta + d \sin(\lambda+1)\theta], \\ \tau_{r\theta} &= \lambda r^{\lambda-1} [(\lambda-1)(a \sin(\lambda-1)\theta - b \cos(\lambda-1)\theta) + c \sin(\lambda+1)\theta - d \cos(\lambda+1)\theta], \end{aligned} \quad (15)$$

in which a, b, c, d are constants, and, for the displacements,

$$\begin{aligned} u_r &= \frac{-r^\lambda}{2\mu} [(\lambda-\kappa)(a \cos(\lambda-1)\theta + b \sin(\lambda-1)\theta) + c \cos(\lambda+1)\theta + d \sin(\lambda+1)\theta], \\ u_\theta &= \frac{r^\lambda}{2\mu} [(\lambda+\kappa)(a \sin(\lambda-1)\theta - b \cos(\lambda-1)\theta) + c \sin(\lambda+1)\theta - d \cos(\lambda+1)\theta], \end{aligned} \quad (16)$$

wherein $\kappa = 3 - 4\nu$.[†]

Now returning to the satisfaction of the cohesive stress-separation law, the second of (9) modifies σ_θ, u_θ of (15), (16) so that

$$\begin{aligned}\sigma_\theta &= \lambda r^{\lambda-1} [(\lambda+1)(a \cos(\lambda-1)\theta + b \sin(\lambda-1)\theta) + c \cos(\lambda+1)\theta - (\lambda-1)b \sin(\lambda+1)\theta], \\ u_\theta &= \frac{r^\lambda}{2\mu} [(\lambda+\kappa)(a \sin(\lambda-1)\theta - b \cos(\lambda-1)\theta) + c \sin(\lambda+1)\theta + (\lambda-1)b \cos(\lambda+1)\theta].\end{aligned}\tag{17}$$

Substituting (17) into the remaining condition in (9) it becomes apparent that the σ_θ and u_θ of (17) cannot interact because of their different powers of r . At first thought, then, it would appear that σ_θ and u_θ must both be independently zero in order to satisfy the first of (9), since this is a homogeneous condition. Unfortunately, such a double requirement can seldom be complied with since, in effect, it realizes a total of *five* boundary conditions and we still have only *four* constants to meet them with. Fortunately, this overly restrictive situation can be alleviated as follows. We do indeed let the quantity with the lower power of r be independently zero. Thus we let σ_θ of (17) by itself be zero. If we then increase λ by one so that $\lambda \rightarrow \lambda+1$, the associated stress can interact with u_θ of (17). However, the $\lambda+1$ field has a u_θ leftover; this displacement in turn must interact with a σ_θ for $\lambda \rightarrow \lambda+2$. And so on. That is, replacing λ by $\lambda+n$, the first of (9) requires:

$$\begin{aligned}\sigma_\theta \Big|_{n=0} &= 0, \\ \sigma_\theta \Big|_n &= k u_\theta \Big|_{n-1}, \quad n = 1, 2, \dots.\end{aligned}\tag{18}$$

[†] For plane stress, $\kappa = (3 - \nu) / (1 + \nu)$.

Straightforward manipulation then yields the following series expansions for σ_θ, u_θ :

$$\begin{aligned}\sigma_\theta &= \sum_{n=0}^{\infty} r^{\lambda+n-1} \mathbf{a}_n \cdot \mathbf{f}_n(\theta), \\ u_\theta &= \sum_{n=0}^{\infty} r^{\lambda+n} \mathbf{b}_n \cdot \mathbf{f}_n(\theta),\end{aligned}\tag{19}$$

where the vectors $\mathbf{a}_n, \mathbf{b}_n, \mathbf{f}_n(\theta)$ are given by

$$\begin{aligned}\mathbf{a}_n &= (\lambda+n)((\lambda+n+1)\mathbf{a}_n, (\lambda+n+1)\mathbf{b}_n, \kappa_n \mathbf{b}_{n-1} - (\lambda+n+1)\mathbf{a}_n, -(\lambda+n-1)\mathbf{b}_n), \\ \mathbf{b}_n &= \frac{1}{2\mu}(-(\lambda+n+\kappa)\mathbf{b}_n, (\lambda+n+\kappa)\mathbf{a}_n, (\lambda+n-1)\mathbf{b}_n, \kappa_n \mathbf{b}_{n-1} - (\lambda+n+1)\mathbf{a}_n), \\ \mathbf{f}_n(\theta) &= (\cos(\lambda+n-1)\theta, \sin(\lambda+n-1)\theta, \cos(\lambda+n+1)\theta, \sin(\lambda+n+1)\theta),\end{aligned}\tag{20}$$

with

$$\kappa_n = \frac{-k(\kappa+1)}{2\mu(\lambda+n)},\tag{21}$$

and the understanding that $b_{-1}=0$ while the other $\mathbf{a}_n, \mathbf{b}_n$ are simply the constants for λ being $\lambda+n, n=0, 1, 2, \dots$.

Substituting the series expansions of (19) into whatever are the outstanding boundary conditions that hold on the other wedge face at $\theta = \phi$ results in a series of 2×2 systems of equations in the constants $\mathbf{a}_n, \mathbf{b}_n$ ($n = 0, 1, 2, \dots$). The first of these is homogeneous. It requires the value of λ be an *eigenvalue* of the problem associated with $n = 0$, and relates b_0 to a_0 . Subsequent systems are inhomogeneous and serve to determine $\mathbf{a}_n, \mathbf{b}_n$ ($n = 1, 2, \dots$).[†]

For $n = 0$, (9) reduces to (see (18))

[†] This is so provided the determinants of the attendant coefficient matrices are not zero - we demonstrate how to handle such systems in Section 4.

$$\sigma_\theta = \tau_{r\theta} = 0. \quad (22)$$

It follows, therefore, that the cohesive stress-separation conditions (9) have an identical influence on the eigenvalues of one of our wedge problems as do the stress-free conditions. Moreover, this can similarly be shown to be true for the dual of (9), namely $k = 0$, $k' \neq 0$. Together, then, these results establish that the boundary conditions for *cohesive stress-separation laws* ((i) of Table 1) are completely *equivalent* to the *stress-free boundary conditions* ((ii) of Table 1) in so far as the eigenvalues of any of our admissible wedge problems are concerned. This means, in particular, that any singular nature present in a wedge with cohesive stress boundary conditions is the same as that present with these conditions exchanged for stress-free boundary conditions.

3. Eigenvalue equations

Here we exploit the equivalence of cohesive stress boundary conditions with stress-free conditions to establish a complete set of *eigenvalue equations* for cohesive stress boundary conditions in combination with any of the other boundary conditions in Table 1. We then examine these equations for possible singular behavior.

As mentioned in Section 2, when cohesive stress boundary conditions hold on $\theta = 0$, the further boundary conditions on $\theta = \phi$ generate a homogeneous 2×2 set of linear algebraic equations in a_0, b_0 . For a nontrivial solution, the coefficient matrix of this set must be singular. Setting the determinant to zero then provides an equation in λ such that this is so, i.e., the eigenvalue equation.

Given the equivalence with respect to eigenvalue equation generation of cohesive stress boundary conditions ((i) of Table 1) with stress-free conditions ((ii) of Table 1), the following distinct pairs of boundary conditions for the angular wedge may be identified. First we have these equivalent conditions paired with themselves:

$$(i) \text{ or } (ii) - (i) \text{ or } (ii). \quad (23)$$

Asymptotic character found for this pairing is the same as results from both its symmetric plus its antisymmetric contributors:

$$(i) \text{ or } (ii) - (iv) \ \& \ (v). \quad (24)$$

Completing possible pairings with (i)/(ii), we have the outstanding set of boundary conditions of Table I, namely

$$(i) \text{ or } (ii) - (iii). \quad (25)$$

The three eigenvalue equations resulting from (24), (25) represent a complete set of all possible combinations of the boundary conditions in Table 1 with cohesive stress boundary conditions. These equations are set out in Table 2 (p. 18).

The eigenvalue equation for (23) is given in Williams [2]; separating it into symmetric and antisymmetric parts yields the first two equations of Table 2. In these equations, ϕ continues as the entire vertex angle so that (iv), (v) have actually been applied on $\theta = \phi / 2$, the wedge bisector. The eigenvalue equation for (25) for plane stress is given in Williams [2] as well; adaptation to the case of plane strain for inclusion in Table 2 is immediate.

Table 2. Eigenvalue equations with cohesive stress boundary conditions

No.	Equation	Applicable boundary conditions, associated vertex angle
I	$\sin \lambda \phi = -\lambda \sin \phi$	(i) - (iv), $\phi / 2$; (i) - (i) or (ii), ϕ
II	$\sin \lambda \phi = \lambda \sin \phi$	(i) - (v), $\phi / 2$; (i) - (i) or (ii), ϕ
III	$(\kappa + 1)^2 = 4(\lambda^2 \sin^2 \phi + \kappa \sin^2 \lambda \phi)$	(i) - (iii), ϕ

In checking for roots of the eigenvalue equations, we are primarily concerned with values of λ that are less than one since these can lead to singularities (see (15) or (19)). For $\lambda = 1$, it is possible to have a logarithmic singularity, so we include this value too (see Dempsey and Sinclair [9] for the full necessary conditions for this possibility). We restrict the search to $\lambda > 0$ so that any such stress singularities are guaranteed to be integrable, viz., to have finite forces. On occasion, eigenvalues can be complex: then the preceding restrictions apply to the real part. Thus, in sum, we confine attention to eigenvalues in the range

$$0 < \text{Re } \lambda \leq 1. \quad (26)$$

Eigenvalues complying with (26) for the three eigenvalue equations of Table 2 are presented in Fig. 5 as a function of wedge vertex angle.

The curves in Fig. 5 display values of the *singularity exponent*, $1 - \lambda$, rather than the eigenvalue itself, λ . The larger the value of this exponent, the more singular are possible vertex stresses. This is because

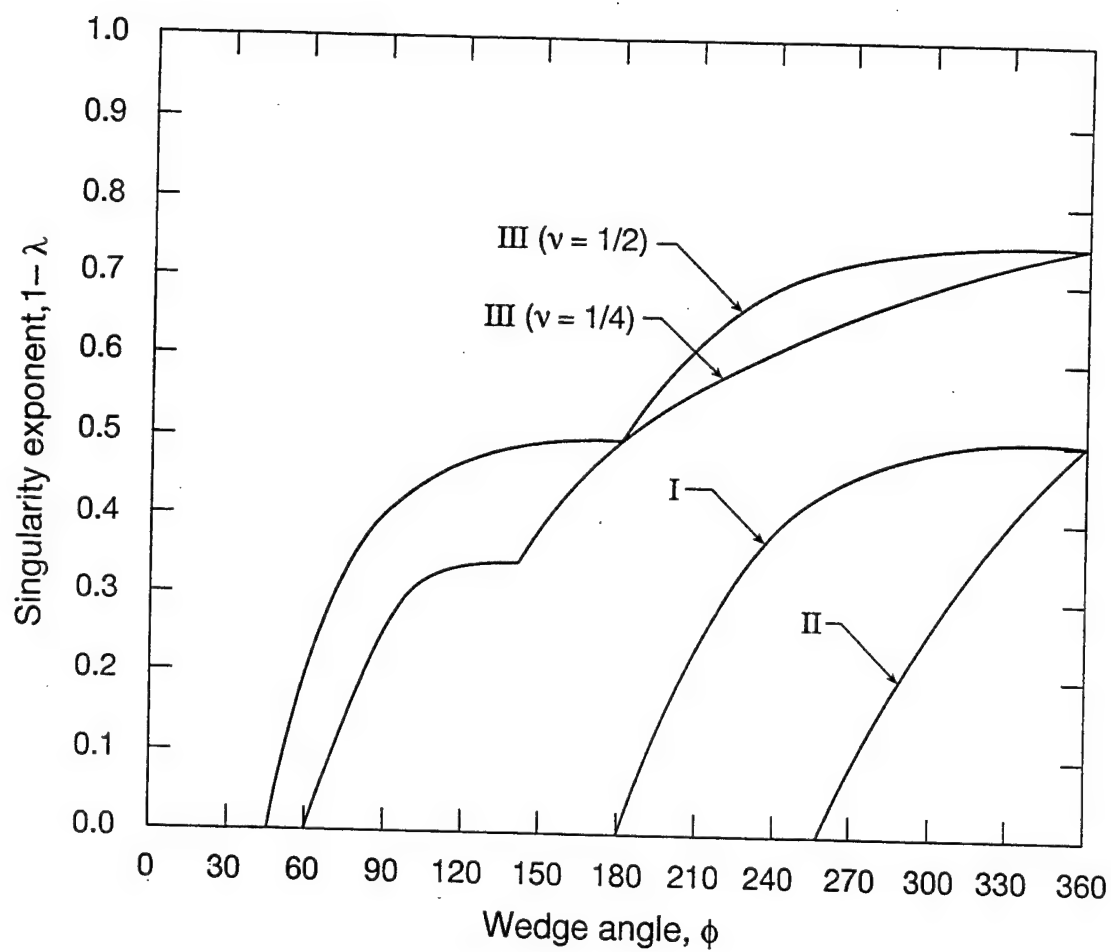


Fig. 5. Singularity exponents for cohesive stress boundary conditions

$$\sigma = O(1/r^{1-\lambda}) \text{ as } r \rightarrow 0, \quad (27)$$

wherein σ is any stress component, σ_r, σ_θ , or $\tau_{r\theta}$ (see (15)). Apparent in Fig. 5, is that the symmetric response, I of Table 2, is uniformly more singular than the antisymmetric, II, for $\phi < 2\pi$. Hence I is the curve shown in Williams [2] for the dominant singular behavior under free-free conditions. Here it is also the dominant singular curve for cohesive stress-separation conditions in concert with either themselves or stress-free conditions. For cohesive stress-separation conditions together with clamped conditions, III, the curve for $\nu = 1/4$ closely follows that given in Williams [2] for clamped-free conditions (the ν used in [2] for plane stress corresponds to $\nu = 3/13$ here for plane strain). The additional case of $\nu = 1/2$ is included for these conditions since it is more singular. For III, for both values of ν , there exist other curves which represent less singular response than that shown in Fig. 5 for a given wedge angle ϕ , yet nonetheless potentially singular stresses.

As well as giving the strength of possible stress singularities, the eigenvalue equations determine when singular behavior is no longer possible. Identifying boundary conditions as in Table 1, these *nonsingular ranges* of vertex angles are as follows. For (i) with (i) or (ii) under symmetric loading, i.e., from I,

$$0 \leq \phi \leq \pi. \quad (28)$$

For (i) with (i) or (ii) under antisymmetric loading, i.e., from II,

$$0 \leq \phi \leq \phi^*, \quad \tan \phi^* = \phi^* \quad (0 < \phi^* < 2\pi). \quad (29)$$

From Abramowitz and Stegun [10], p. 224, $\phi^* = 257.45^\circ$. For (i) with (iii), i.e., from III,

$$0 \leq \phi \leq \sin^{-1} \sqrt{\kappa + 1} / 2, \quad (30)$$

with the understanding that the inverse sine takes its principal value. For $\nu = 1/4, 1/2$, $\kappa = 3 - 4\nu$ takes on the values 2, 1, and (30) gives $\phi \leq \pi/3, \pi/4$, respectively, as shown in Fig. 5.

Given the equivalence of boundary conditions for cohesive stress-separation laws with stress-free conditions, the above ranges are the *same* as for free-free and clamped-free wedges. How, then, does the use of cohesive stress boundary conditions lower the number of instances of singular behavior? There are two ways. For free-free wedges, one can introduce cohesive stress conditions on an *interior* ray within a given wedge, a ray upon which it is reasonable to consider the possibility of failure: thus the effective wedge angle is reduced and more likely to fall within the nonsingular ranges of (28), (29). For clamped-free wedges, one may be able to replace the clamped conditions with cohesive stress conditions: hence the range of nonsingular wedge angles goes from (30) to (28) or (29) and nonsingular response is more likely. We demonstrate these two ways in the next section.

4. Eigenfunctions for some special cases

Here we consider the effects of introducing cohesive stress-separation laws for some specific local features. The particular configurations examined are: a crack tip under symmetric (mode I) loading (Fig. 6a), a reentrant corner subjected to symmetric loading (Fig. 6b), an epoxy-steel butt joint under tension (Fig. 6c), and a junction of three phases in a titanium aluminide microstructure (Fig. 6d). In what follows, we treat each of these instances in turn, and compare local stresses with and without cohesive laws.

For the perfectly sharp *crack* under mode I loading, symmetry enables attention to be confined to the upper half-plane. For this half-plane, classical boundary

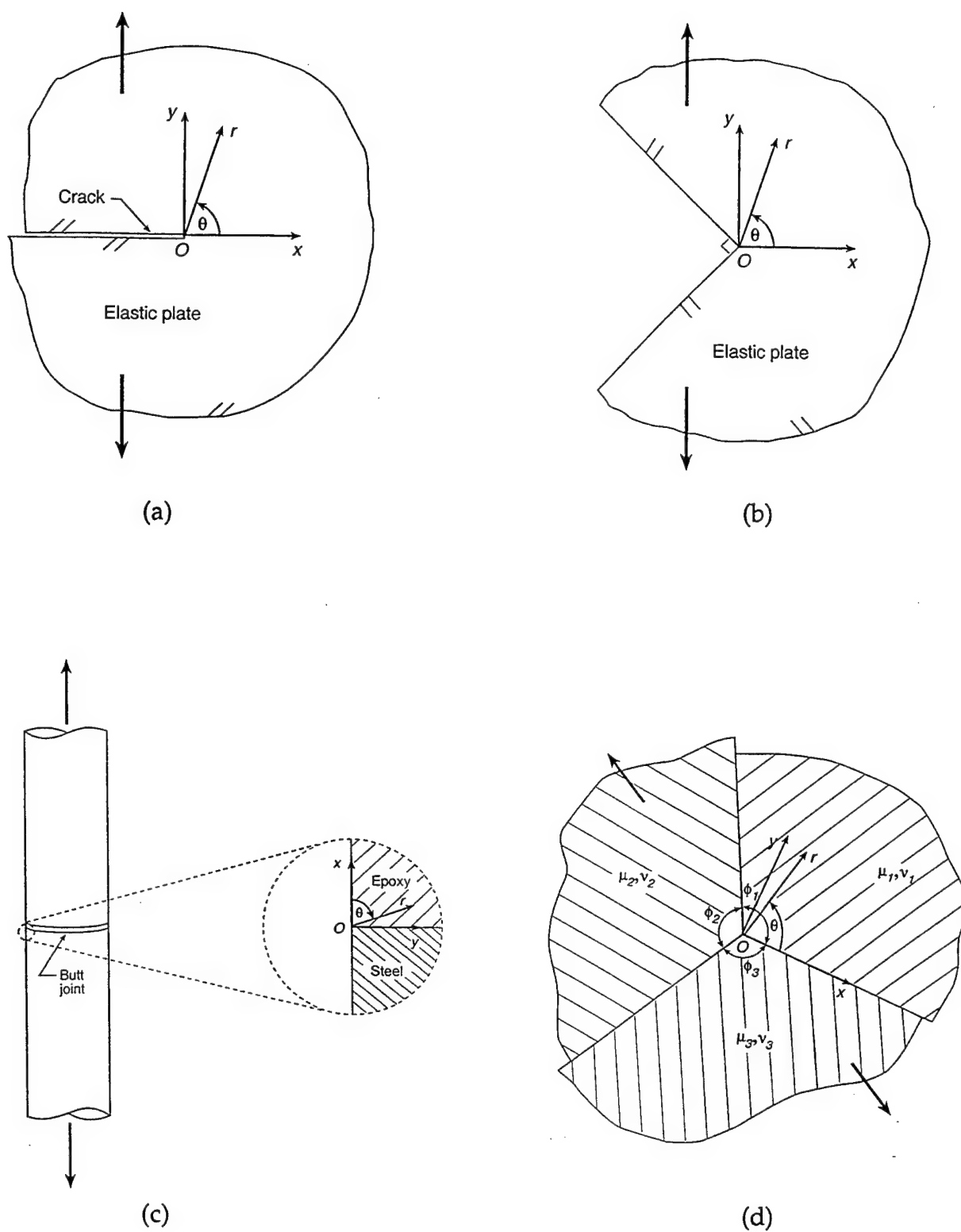


Fig. 6. Some special cases: (a) crack tip, (b) reentrant corner, (c) epoxy-steel butt joint and (d) junction of phases in TiAl microstructure

conditions take stress-free conditions on the crack flank, symmetry conditions ahead of the crack. That is, for the coordinate system of Fig. 6a,

$$\begin{aligned}\sigma_\theta = \tau_{r\theta} = 0 \quad \text{at} \quad \theta = \pi, \\ u_\theta = 0, \quad \tau_{r\theta} = 0 \quad \text{at} \quad \theta = 0,\end{aligned}\tag{31}$$

for $0 < r < \infty$. Using the equivalence with respect to eigenvalue equations of stress-free boundary conditions with cohesive, the associated eigenvalue equation may be taken from Table 2 as I with $\phi = 2\pi$, and is :

$$\sin 2\pi\lambda = 0.\tag{32}$$

Consequently the dominant singularity admitted (recall (26)) has $\lambda = 1/2$ and

$$\sigma = O(1/\sqrt{r}) \quad \text{as} \quad r \rightarrow 0,\tag{33}$$

wherein σ continues as any stress component.[†] This is the classical, inverse-square-root, stress singularity of present day fracture mechanics.

With Barenblatt's approach [4], cohesive stresses are introduced on the crack flank while symmetry conditions are maintained ahead of the crack. Given symmetry, these boundary conditions are

$$\begin{aligned}\sigma_\theta = -2ku_\theta, \quad \tau_{r\theta} = 0 \quad \text{at} \quad \theta = \pi, \\ u_\theta = 0, \quad \tau_{r\theta} = 0 \quad \text{at} \quad \theta = 0,\end{aligned}\tag{34}$$

[†] Details of these local fields are well known and may be found, for example, in Rice [7] at p. 216.

for $0 < r < \infty$. The minus sign in (34) is simply an outcome of applying the cohesive conditions on $\theta = \pi$, and the 2 reflects the total separation of the crack faces under symmetric loading. In the light of the equivalence of the cohesive conditions in (34) to the stress-free conditions in (31), we have the same eigenvalue equation for this configuration, to wit (32), and same singular character, to wit (33). Now, though, there are two instigators of singular stress fields: one being far-field loading, the other being the cohesive stresses on the crack flank. Since these share the same singular character, they can be adjusted to cancel one another, as in Barenblatt [4].

Here, instead, we introduce cohesive laws both behind and ahead of the crack tip (as in Fig. 2). That is, our local boundary conditions for symmetric loading are

$$\sigma_\theta = -2ku_\theta, \quad \tau_{r\theta} = 0 \quad \text{at} \quad \theta = \pi, \quad (35)$$

$$\sigma_\theta = 2ku_\theta, \quad \tau_{r\theta} = 0 \quad \text{at} \quad \theta = 0,$$

for $0 < r < \infty$. The eigenvalue equation for these conditions is still I of Table 2, but now with $\phi = \pi$, i.e.,

$$\sin \lambda\pi = 0. \quad (36)$$

This is an example of the reduction in effective wedge angle mentioned at the close of Section 3. Eigenvalues with integrable stresses as a result become

$$\lambda = 0, 1, 2, \dots \quad (37)$$

None of the associated stress fields are singular (the $\lambda = 0$ field corresponds to a rigid body displacement). However, we do have the situation mentioned earlier, namely that

successive coefficient matrices for assembling eigenfunction series expansions are themselves singular. Fortunately, by combining rigid body displacement fields with simple polynomial solutions for the stresses, we can construct eigenfunctions which are not series. These are most succinctly expressed in rectangular coordinates (Fig. 6a), and take the following forms: for the stresses,

$$\begin{aligned}\sigma_y &= 2k \left[v_0 + v_1 \frac{x}{a} + v_2 \left(\frac{x}{a} \right)^2 + O(x^3) \right], \\ \sigma_x &= -2kv_2 \frac{y}{a} \left[\frac{y}{a} + \frac{8\mu}{(1+\kappa)ka} \right] + O(xy),\end{aligned}\tag{38}$$

as $x \rightarrow 0$, $y/a \ll 1$, while for the displacements

$$\begin{aligned}v &= \left[v_0 + v_1 \frac{x}{a} \right] \left[1 + \frac{(1+\kappa)ky}{4\mu} \right] \\ &\quad + \frac{v_2}{a^2} \left[x^2 + \frac{3-\kappa}{1+\kappa} y^2 + \frac{ky}{12\mu} (3(1+\kappa)x^2 + (3-\kappa)y^2) \right] + O(xy^2) + O(x^3),\end{aligned}\tag{39}$$

$$\begin{aligned}u &= -v_0 \frac{(3-\kappa)kx}{4\mu} - \frac{v_1}{a} \left[y + \frac{k}{8\mu} ((3-\kappa)x^2 + (1+\kappa)y^2) \right] \\ &\quad - \frac{2v_2x}{a^2} \left[y + \frac{k}{8\mu} (3(3-\kappa)x^2 + (1+\kappa)y^2) \right] + O(y^3) + O(x^2y),\end{aligned}$$

as $x \rightarrow 0$, $y/a \ll 1$. In (38), (39), $2a$ remains the crack length, v_0 , v_1 , v_2 are arbitrary displacements in the y -direction, and the shear stress associated with these coefficients is everywhere zero. This is not the case in general, however. For example, the

companion shear stress for $\sigma_y = kv_3(x/a)^3$ has terms of ord (v_3y^3) and ord (v_3y^2) as $x \rightarrow 0$.[†] The above fields may be verified directly by substituting them into the stress equations of equilibrium, the stress-displacement relations, and the boundary conditions (35) on converting to rectangular coordinates; when this is done, the fields in (38), (39), together with $\tau_{xy} = 0$, are indeed found to satisfy all these requirements. They can also be augmented by the fields associated with $\sigma_x = \text{constant}$, $\sigma_y = \tau_{xy} = 0$. With or without these last, clearly the fields in (38), (39) are *not singular*.

For the closely related configuration of a 90° *reentrant corner* subjected to symmetric loading (Fig. 6b), classical boundary conditions for the upper half of the plate have stress-free conditions on the inclined face together with symmetry conditions ahead of the corner. That is

$$\begin{aligned}\sigma_\theta = \tau_{r\theta} = 0 \quad \text{at} \quad \theta = 3\pi/4, \\ u_\theta = 0, \quad \tau_{r\theta} = 0 \quad \text{at} \quad \theta = 0,\end{aligned}\tag{40}$$

for $0 < r < \infty$. Thus the eigenvalue equation is (from Table 2 as I with $\phi = 3\pi/2$),

$$\sin \frac{3\pi\lambda}{2} = \lambda.\tag{41}$$

Solving (41) numerically for λ within the range 0-1 yields $\lambda = 0.544$. Hence singular stresses of order

$$\sigma = O(r^{-0.456}) \quad \text{as} \quad r \rightarrow 0\tag{42}$$

[†] Herein the ord notation implies that, if $f(x) = \text{ord}(ax^\alpha)$ as $x \rightarrow 0$, a and α being independent of x , then in fact $f(x) = kax^\alpha$ as $x \rightarrow 0$ with the multiplicative constant k *not* being zero. This is in contrast to the O notation which admits the possibility of k being zero.

are possible in the corner. Thus the singular character here is only a little weaker than that for the crack.

Now introducing cohesive laws between the upper and lower halves of the plate with a reentrant corner, the boundary conditions become:

$$\begin{aligned}\sigma_{\theta} = -\tau_{r\theta} &= \frac{k}{\sqrt{2}}(r + u_r - u_{\theta}) \quad \text{at } \theta = 3\pi/4, \\ \sigma_{\theta} &= 2ku_{\theta}, \quad \tau_{r\theta} = 0 \quad \text{at } \theta = 0,\end{aligned}\tag{43}$$

for $0 < r < \infty$. These conditions take the vertical traction on the corner faces to be k times the *total* separation of the faces due to their angle and to any vertical displacement. They also take the horizontal traction to be zero since there is no relative horizontal displacement between the upper and lower halves of the plate because of symmetry. From Table 2, the eigenvalue equations for these conditions are I and II with $\phi = 3\pi/4$, viz.,

$$\sin \frac{3\pi\lambda}{4} = \pm \frac{\lambda}{\sqrt{2}}.\tag{44}$$

Again the wedge angle is effectively reduced. Real eigenvalues with integrable stresses then are

$$\lambda = 0, 1,\tag{45}$$

the first of these corresponding to a rigid body displacement field. Complex eigenvalues are also possible. These occur in pairs as complex conjugates. The complex pair with the smallest positive real part may be determined numerically and is

$$\lambda = \xi + i\eta, \quad \xi = 1.885, \quad \eta = \pm 0.361. \quad (46)$$

The next complex root has $\xi > 3$, and further roots have still greater real parts. Thus *none* of the eigenvalues of (44) lead to singular stress fields. The series expansions for the associated eigenfunctions can be constructed in the manner outlined in Section 2. After some algebra, this yields: for the stresses,

$$\sigma_r = 2kv_0 \sin^2 \theta$$

$$-\frac{kr}{2} \left[\left(1 + \frac{v_0}{a'} - \frac{v_1}{a} \right) \cos \theta + \left(3 + 3 \frac{v_0}{a'} + \frac{v_1}{a} \right) \cos 3\theta \right. \\ \left. + 2 \left(1 + \frac{v_0}{a'} \right) (\sin \theta + \sin 3\theta) \right] + \text{ord}(r^2)$$

$$-\left\{ \frac{v_2 \text{Re}}{v_2' \text{Im}} \right\} \left\{ \left(\frac{r}{a} \right)^{\lambda-1} [(\lambda-1)(\lambda-3) \cos(\lambda-1)\theta - (\lambda^2-1) \cos(\lambda+1)\theta \right. \\ \left. + (\sqrt{2-\lambda^2}+1)((\lambda-3) \sin(\lambda-1)\theta - (\lambda-1) \sin(\lambda+1)\theta)] + \text{ord}(r^\lambda) \right\},$$

$$\sigma_\theta = 2kv_0 \cos^2 \theta$$

$$-\frac{kr}{2} \left[3 \left(1 + \frac{v_0}{a'} - \frac{v_1}{a} \right) \cos \theta - \left(3 + 3 \frac{v_0}{a'} + \frac{v_1}{a} \right) \cos 3\theta \right. \\ \left. + 2 \left(1 + \frac{v_0}{a'} \right) (3 \sin \theta - \sin 3\theta) \right] + \text{ord}(r^2)$$

(47)

$$+\left\{ \frac{v_2 \text{Re}}{v_2' \text{Im}} \right\} \left\{ \left(\frac{r}{a} \right)^{\lambda-1} [(\lambda^2-1)(\cos(\lambda-1)\theta - \cos(\lambda+1)\theta) \right. \\ \left. + (\sqrt{2-\lambda^2}+1)((\lambda+1) \sin(\lambda-1)\theta - (\lambda-1) \sin(\lambda+1)\theta)] + \text{ord}(r^\lambda) \right\},$$

$$\tau_{r\theta} = 2kv_0 \sin\theta \cos\theta$$

$$-\frac{kr}{2} \left[\left(1 + \frac{v_0}{a'} - \frac{v_1}{a} \right) \sin\theta - \left(3 + 3\frac{v_0}{a'} + \frac{v_1}{a} \right) \sin 3\theta \right. \\ \left. + 2 \left(1 + \frac{v_0}{a'} \right) (\cos 3\theta - \cos\theta) \right] + \text{ord}(r^2)$$

$$+ \left\{ \frac{v_2 \text{Re}}{v_2' \text{Im}} \right\} \left\{ \left(\frac{r}{a} \right)^{\lambda-1} (\lambda-1) [(\lambda-1)\sin(\lambda-1)\theta - (\lambda+1)\sin(\lambda+1)\theta \right. \\ \left. + (\sqrt{2-\lambda^2}+1)(\cos(\lambda+1)\theta - \cos(\lambda-1)\theta) \right\} + \text{ord}(r^\lambda) \Big\},$$

as $r \rightarrow 0$, $0 \leq \theta \leq 3\pi/4$, while for the displacements

$$u_r = v_0 \sin\theta + \frac{rv_0}{(1+\kappa)a'} [\kappa - 1 - 2\cos 2\theta]$$

$$+ \text{ord}(r^2) + \text{ord}(v_2 r^\lambda) + \text{ord}(v_2' r^\lambda),$$

$$u_\theta = v_0 \cos\theta + r \left[\frac{2v_0}{(1+\kappa)a'} \sin 2\theta + \frac{v_1}{a} \right] \quad (48)$$

$$+ \text{ord}(r^2) + \text{ord}(v_2 r^\lambda) + \text{ord}(v_2' r^\lambda),$$

as $r \rightarrow 0$, $0 \leq \theta \leq 3\pi/4$. In (47), (48), a is now the depth of the reentrant corner, a' is a further normalizing length defined by $a' = 4\mu/k(1+\kappa)$, v_0, v_1, v_2 continue as arbitrary displacements supplemented by v_2' , and λ satisfies (44) with the minus sign with its actual value being either of the complex roots given in (46). These fields may be verified directly by substitution into the governing field equations, namely (7), (8) together with stress compatibility, $\nabla^2(\sigma_r + \sigma_\theta) = 0$, for the higher order stress terms,

and the boundary conditions (43). When this check is performed, the fields in (47), (48) are indeed found to comply with all these requirements. In the interests of brevity, we terminate explicit expressions for series terms in these fields at ord (r) and simply give the orders of the next terms: other than the somewhat lengthy algebra involved, there would not appear to be any impediment to determining these higher order terms explicitly. As before, clearly the fields in (47), (48) are *not singular*.

Turning to the *epoxy-steel interface* where it meets the outside free surface of the composite tensile specimen (Fig. 6c), in view of the relative rigidity of steel compared to epoxy, classical boundary conditions for the elastic response of the epoxy are clamped-free:

$$u_r = u_\theta = 0 \quad \text{at} \quad \theta = \pi / 2, \quad (49)$$

$$\sigma_\theta = \tau_{r\theta} = 0 \quad \text{at} \quad \theta = 0,$$

for $0 < r < \infty$. If the composite specimen is thick in the out-of-plane direction in Fig. 6c, the appropriate field equations are those of plane strain, i.e., (7), (8). Even if the specimen is the normal cylindrical one used in practice, these field equations are still appropriate for examining local behavior (see Aksentian [8]). Hence, given the equivalence of stress-free conditions with cohesive, the pertinent eigenvalue equation can be drawn from Table 2 as III with $\phi = \pi / 2$. That is,

$$(\kappa + 1)^2 = 4 \left(\lambda^2 + \kappa \sin^2 \frac{\pi \lambda}{2} \right). \quad (50)$$

For epoxy, a representative value of Poisson's ratio is $3/8$ corresponding to $\kappa = 3/2$. Then solving (50) numerically for λ within the range 0-1 furnishes $\lambda = 2/3$, and the dominant singularity possible has

$$\sigma = O(r^{-1/3}) \text{ as } r \rightarrow 0. \quad (51)$$

This is a weaker singularity than for either of the previous two configurations, but quite a strong one nonetheless.

Now instead we introduce a cohesive law between the epoxy and relatively rigid steel. The resulting boundary conditions are taken to be:

$$\sigma_\theta = -ku_\theta, \quad u_r = 0 \quad \text{at } \theta = \pi/2, \quad (52)$$

$$\sigma_\theta = \tau_{r\theta} = 0 \quad \text{at } \theta = 0,$$

for $0 < r < \infty$. In (52), we have only incorporated a cohesive stress-separation law normal to the interface and not admitted the possibility of relative tangential displacements between the epoxy and the steel. This choice is arguably the simplest model; however, one could quite reasonably also introduce a cohesive law for tangential displacements. Given the equivalence of the very first of (52) with the condition $\sigma_\theta = 0$, these conditions in their entirety realize the same boundary conditions as for a complete half-plane under antisymmetric loading. From Table 2, the eigenvalue equation is thus Π with $\phi = \pi$, viz.,

$$\sin \lambda\pi = 0. \quad (53)$$

Associated eigenvalues with integrable stresses are

$$\lambda = 0, 1, 2, \dots \quad (54)$$

The first of these continues to correspond to a rigid body displacement field. Since the other eigenvalues are separated by integers, we have the situation alluded to in Section 2 wherein coefficient matrices for assembling further terms in eigenfunction expansions are themselves singular. To overcome this difficulty, we need to develop auxiliary fields to those of (15), (16); this is done by successive differentiation of the expressions in (15), (16) with respect to λ . Details of the fields so formed are set out in the Appendix. These fields enable eigenfunction expansions to be constructed. The algebra involved is somewhat lengthy, but straightforward. The end result as far as the stresses go is:

$$\begin{aligned}
 \sigma_r = & \bar{k}u_0[\pi(\kappa-1)(1+\cos 2\theta) + (3-\kappa)(2\theta + \sin 2\theta)] \\
 & - \bar{k}r(3-\kappa) \left\{ \left[\frac{\bar{k}u_0}{\mu} (2 + \kappa'(1 - 4\kappa''\theta + 2\theta^2)) - \frac{u_1}{2a} - \frac{u'_1}{a} \right] \cos \theta \right. \\
 & \quad - \left[\frac{\bar{k}u_0}{\mu} (10 - \kappa'(3 - 4\kappa''\theta + 6\theta^2)) - \frac{5u_1}{2a} + 3\frac{u'_1}{a} \right] \cos 3\theta \\
 & \quad - \left[\frac{\bar{k}u_0}{\mu} (3\pi - 4\kappa'\kappa'' - 4\theta(1 - \kappa')) - \frac{u_1}{a}(\kappa'' - \theta) \right] \sin \theta \\
 & \quad - \left[\frac{\bar{k}u_0}{\mu} (3\pi + 4\kappa'\kappa'' - 4\theta(3 + \kappa')) - \frac{u_1}{a}(\kappa'' - 3\theta) \right] \sin 3\theta \\
 & \quad - \ln r \left[\left(4\frac{\bar{k}u_0}{\mu}(1 - \kappa') - \frac{u_1}{a} \right) \cos \theta + \left(4\frac{\bar{k}u_0}{\mu}(3 + \kappa') - 3\frac{u_1}{a} \right) \cos 3\theta \right. \\
 & \quad \quad \left. + 4\kappa' \frac{\bar{k}u_0}{\mu} ((\kappa'' - \theta) \sin \theta + (\kappa'' - 3\theta) \sin 3\theta) \right] \\
 & \quad \left. - 2\kappa' \frac{\bar{k}u_0}{\mu} (\ln r)^2 (\cos \theta + 3 \cos 3\theta) \right\} \\
 & + \text{ord}(u_0 r^2 (\ln r)^3) + \text{ord}(u_1 r^2 (\ln r)^2) + \text{ord}(u'_1 r^2 \ln r),
 \end{aligned}$$

$$\begin{aligned}
\sigma_\theta = & \bar{k}u_0[\pi(\kappa-1)(1-\cos 2\theta) + (3-\kappa)(2\theta - \sin 2\theta)] \\
& + \bar{k}r(3-\kappa) \left\{ \left[\frac{\bar{k}u_0}{\mu} (10 - 3\kappa' - 6\kappa'\theta^2) - \frac{5u_1}{2a} + 3\frac{u_1'}{a} \right] (\cos \theta - \cos 3\theta) \right. \\
& \quad + 4\kappa'\kappa'' \frac{\bar{k}u_0}{\mu} \theta (3\cos \theta - \cos 3\theta) \\
& \quad + \left[\frac{\bar{k}u_0}{\mu} (9\pi + 4\kappa'\kappa'' - 4\theta(3+\kappa')) - 3\frac{u_1}{a} (\kappa'' - \theta) \right] \sin \theta \\
& \quad - \left[\frac{\bar{k}u_0}{\mu} (3\pi + 4\kappa'\kappa'' - 4\theta(3+\kappa')) - \frac{u_1}{a} (\kappa'' - 3\theta) \right] \sin 3\theta \\
& \quad + \ln r \left[\left(4\frac{\bar{k}u_0}{\mu} (3+\kappa') - 3\frac{u_1}{a} \right) (\cos \theta - \cos 3\theta) \right. \\
& \quad \quad \left. + 4\kappa' \frac{\bar{k}u_0}{\mu} (3(\kappa'' - \theta) \sin \theta - (\kappa'' - 3\theta) \sin 3\theta) \right] \\
& \quad \left. + 6\kappa' \frac{\bar{k}u_0}{\mu} (\ln r)^2 (\cos \theta - \cos 3\theta) \right\} \\
& + \text{ord}(u_0 r^2 (\ln r)^3) + \text{ord}(u_1 r^2 (\ln r)^2) + \text{ord}(u_1' r^2 \ln r),
\end{aligned} \tag{55}$$

$$\begin{aligned}
\tau_{r\theta} = & -\bar{k}u_0[\pi(\kappa-1)\sin 2\theta + (3-\kappa)(1-\cos 2\theta)] \\
& - \bar{k}r(3-\kappa) \left\{ \left[\frac{\bar{k}u_0}{\mu} (3\pi + 4\kappa'(\kappa'' - \theta)) - \kappa'' \frac{u_1}{a} \right] (\cos \theta - \cos 3\theta) \right. \\
& \quad - \left(4\frac{\bar{k}u_0}{\mu} - \frac{u_1}{a} \right) \theta (\cos \theta - 3\cos 3\theta) \\
& \quad - \left[\frac{\bar{k}u_0}{\mu} (6 - \kappa' + 2\kappa'\theta(2\kappa'' - \theta)) - \frac{3u_1}{2a} + \frac{u_1'}{a} \right] \sin \theta \\
& \quad + \left[\frac{\bar{k}u_0}{\mu} (10 - 3\kappa' + 2\kappa'\theta(2\kappa'' - 3\theta)) - \frac{5u_1}{2a} + 3\frac{u_1'}{a} \right] \sin 3\theta \\
& \quad + \ln r \left[4\kappa' \frac{\bar{k}u_0}{\mu} (\kappa'' (\cos \theta - \cos 3\theta) - \theta (\cos \theta - 3\cos 3\theta)) \right. \\
& \quad \quad \left. - \left(4\frac{\bar{k}u_0}{\mu} (1+\kappa') - \frac{u_1}{a} \right) \sin \theta + \left(4\frac{\bar{k}u_0}{\mu} (3+\kappa') - 3\frac{u_1}{a} \right) \sin 3\theta \right] \\
& \quad \left. - 2\kappa' \frac{\bar{k}u_0}{\mu} (\ln r)^2 (\sin \theta - 3\sin 3\theta) \right\} \\
& + \text{ord}(u_0 r^2 (\ln r)^3) + \text{ord}(u_1 r^2 (\ln r)^2) + \text{ord}(u_1' r^2 \ln r),
\end{aligned}$$

as $r \rightarrow 0$, $0 \leq \theta \leq \pi/2$. Companion displacements are:

$$\begin{aligned}
 u_r &= u_0 \left\{ \cos \theta + \frac{\bar{k}r}{4\mu} \left[\pi(\kappa - 1)(2 \cos 2\theta + \kappa - 1) + 2(3 - \kappa)(\sin 2\theta + (\kappa - 1)\theta) \right] \right\} \\
 &\quad + \text{ord}(u_0 r^2 (\ln r)^2) + \text{ord}(u_1 r^2 \ln r) + \text{ord}(u_1' r^2), \\
 u_\theta &= -u_0 \left\{ \sin \theta + \frac{\bar{k}r}{2\mu} \left[\pi(\kappa - 1) \sin 2\theta + (3 - \kappa)(1 - \cos 2\theta + (1 + \kappa) \ln r) \right] \right\} \\
 &\quad + \frac{u_1 r}{a} + \text{ord}(u_0 r^2 (\ln r)^2) + \text{ord}(u_1 r^2 \ln r) + \text{ord}(u_1' r^2),
 \end{aligned} \tag{56}$$

as $r \rightarrow 0$, $0 \leq \theta \leq \pi/2$. In (55), (56), u_0, u_1, u_1' are arbitrary displacements in the x -direction, a is now any normalizing length, and $\bar{k}, \kappa', \kappa''$ are given by:

$$\bar{k} = k / \pi(1 + \kappa), \quad \kappa' = (3 - \kappa)(1 + \kappa) / 8, \quad \kappa'' = \pi(5 - \kappa) / 2(3 - \kappa). \tag{57}$$

These fields may be verified directly by substituting them into the governing field equations and the boundary conditions (52). Performing this check shows that the fields in (55), (56) in fact meet all of these requirements. Clearly, too, the stresses of (55) are also *free from any singularities*.

As our final example we consider the stress intensification that can occur within the microstructure of titanium aluminide alloys. For the TiAl-base lamellar alloy designated as K5 in Larsen et al. [11], *junctions of phases* with different orientations are not unusual (see Figure 1 (b) in [11]). Such a feature is sketched in Fig. 6d. Herein the different alignments of the anisotropic phases effectively presents different moduli to the interfaces involved when response is in the elastic regime. In Fig. 6d, we have simply designated these different moduli as μ_i, ν_i ($i = 1, 2, 3$) for each of the three phases included in our example. In reality the situation is more complex than this, but

this simplified approach serves to demonstrate the differences between response with and without cohesive laws.

Classical boundary conditions for three distinct elastic materials sharing three interfaces assume continuity of stresses and displacements at an interface, i.e., that the materials are perfectly bonded to one another. For the geometry and coordinates of Fig. 6d, these conditions may be expressed as:

$$\begin{aligned} \sigma_\theta \Big|_{\theta=0^+} &= \sigma_\theta \Big|_{\theta=0^-}, & \tau_{r\theta} \Big|_{\theta=0^+} &= \tau_{r\theta} \Big|_{\theta=0^-}, \\ u_r \Big|_{\theta=0^+} &= u_r \Big|_{\theta=0^-}, & u_\theta \Big|_{\theta=0^+} &= u_\theta \Big|_{\theta=0^-}, \end{aligned} \quad (58)$$

for $0 < r < \infty$, with companion matching conditions on $\theta = \phi_1, \phi_1 + \phi_2$. In (58), $\theta = 0^+$ denotes the limit $\theta \rightarrow 0, \theta > 0$, while $\theta = 0^-$ denotes the limit $\theta \rightarrow 0, \theta < 0$. Unfortunately no full asymptotic analysis of such a trimaterial junction is available in the literature. However, by considering some limiting cases, we can approximately gauge the range of possible singular behavior. To this end, set $\mu_1 = \mu_2$, $\nu_1 = \nu_2 = \nu_3$, then consider the two limits

$$\mu_3 / \mu_1 \rightarrow 0, \quad \mu_3 / \mu_1 \rightarrow \infty. \quad (59)$$

For the first, μ_3 vanishing lets the edges of the combined $\mu_1 - \mu_2$ wedge approach being "stress-free". Thus from Williams [2], if $\phi_1 + \phi_2 > \pi$, we have possible singular response of the form

$$\sigma = O(1/r^{1-\lambda}) \quad \text{as } r \rightarrow 0, \quad 1/2 \leq \lambda < 1. \quad (60)$$

For the second, μ_3 becoming absolutely rigid renders the edges of the combined $\mu_1 - \mu_2$ wedge "clamped", and again from Williams [2], if $\phi_1 + \phi_2 >$ upper value of ϕ in (30), we have singular behavior of the type indicated in (60). Note, though, that the precise values of λ entailed, while falling within the range given in (60), are not generally equal for these two cases. In between the μ_3 of (59), we have the instance of $\mu_3 = \mu_1$ for which there is no singularity. Hence, in all, we can expect singular response with classical boundary conditions for the trimaterial junction depicted in Fig. 6d to vary from being as strong as the inverse-square-root singularity of the classical crack, to being nonsingular, depending upon material properties.

Now we introduce cohesive laws on the interface. That is, we take

$$\sigma_\theta = ku_\theta, \quad \tau_{r\theta} = k'u_r \quad \text{on } \theta = 0, \quad (61)$$

for $0 < r < \infty$, with analogous conditions on $\theta_1 = \phi_1$, $\phi_1 + \phi_2$. Herein u_θ, u_r are total displacements measured across the interface. Thus, in the light of our earlier result that these conditions are equivalent to stress-free ones, we in essence have three stress-free wedges so far as singularities go. Provided each of these "wedges" has a proud corner, i.e., $\phi_i < \pi$, $i = 1, 2, 3$, then the response is nonsingular - recall (28), (29).[†] Moreover, this result holds irrespective of the values of material constants.

Concluding remarks

The examples of Section 4 represent four demonstrations of configurations which promote singular stresses when treated with classical boundary conditions, yet which are nonsingular when cohesive stress-separation laws are introduced. Other examples exist. Accordingly, since singular stresses are rubbish physically, the introduction of

[†] In the event that one or more of the "wedges" has a reentrant corner, the configuration can still be rendered singularity free by the introduction of cohesive conditions within such wedges on rays upon which it is physically appropriate to entertain failure (cf., the earlier reentrant corner example).

cohesive boundary conditions would appear to offer a means of significantly improving modelling in solid mechanics.

The underlying reasons for this alleviation of singular behavior may be described as follows. Cohesive stress-separation laws are fundamental to continuum mechanics in that they represent the solid state physics at the atomic/molecular level which ultimately leads to the constitutive relations for the continuum. As a consequence, when boundaries in the continuum approach one another to within the distances over which the stress-separation laws are active, consistent modelling *requires* the introduction of cohesive stress-separation laws in the boundary conditions. Such is the case for the crack flanks of the mathematically sharp crack. Not to insert cohesive conditions on these crack flanks is, in effect, setting the stiffness in the cohesive law to zero there. This realizes an abrupt discontinuity in the effective stiffness from that taken ahead of the crack, and it is this nonphysical discontinuity which in turn produces singular stresses. However, merely introducing cohesive conditions on the crack flanks and taking, for example, symmetry conditions ahead of the crack (in essence as in Barenblatt [4]) also represents the introduction of a discontinuity in cohesive law stiffness. This is because, when the transverse displacement ahead of the crack is set to zero in the symmetry conditions, the stiffness is effectively being taken as infinite, in contrast to its finite value on the crack flanks. Again such a nonphysical discontinuity produces singular response. Only when a cohesive law is introduced consistently along the crack plane (as in Fig. 2) are such discontinuities avoided and nonsingular stresses result. The same sort of argument is directly applicable to the reentrant corner example treated herein.

In general, the removal of singular stresses stems from the *consistent* employment of cohesive stress-separation laws as boundary conditions. This consistency must exist between the cohesive stress-separation law and the constitutive relations of the continuum, as well as within the cohesive boundary conditions themselves.

References

1. M. Knein, "Zur Theorie des Druckversuchs," *Zeitschrift fur angewandte Mathematik und Mechanik*, **6**, pp. 414-416 (1926).
2. M.L. Williams, "Stress singularities resulting from various boundary conditions in angular corners of plates in extension," *Journal of Applied Mechanics*, **19**, pp. 526-528 (1952).
3. G.B. Sinclair, "Structural reliability through fracture mechanics," *Mechanical Engineering*, **116**, No. 6, pp. 79-84 (1993).
4. G.I. Barenblatt, "The mathematical theory of equilibrium cracks in brittle fracture," *Advances in Applied Mechanics*, **7**, pp. 55-129 (1962).
5. H. Tada, P.C. Paris and G.R. Irwin, *The Stress Analysis of Cracks Handbook* (second edition), Paris Productions Incorporated, St. Louis, Missouri (1985).
6. J.N. Goodier, "Mathematical theory of equilibrium cracks," in *Fracture, An Advanced Treatise* (editor H. Liebowitz), Academic Press, New York, N.Y., **2**, pp. 1-66 (1968).
7. J. R. Rice, "Mathematical analysis in the mechanics of fracture," *ibid* [6], pp. 191-311 (1968).
8. O.K. Aksentian, "Singularities of the stress-strain state of a plate in the neighborhood of an edge," *Prikladnaya Matematika i Mekhanika*, **31**, pp. 193-202 (1967).
9. J.P. Dempsey and G.B. Sinclair, "On the stress singularities in the plane elasticity of the composite wedge," *Journal of Elasticity*, **9**, pp. 373-391 (1979).
10. M. Abramowitz and I.A. Stegun (editors), *Handbook of Mathematical Functions*, Dover Publications Incorporated, New York, N.Y. (1968).
11. J.M. Larsen, B.D. Worth, S.J. Balsone and J.W. Jones, "An overview of the structural capability of available gamma titanium aluminide alloys," in *Gamma Titanium Aluminides* (editors Y-W. Kim, R. Wagner and M. Yamaguchi), TMS/ASM International, U.S.A. (1995).
12. S.P. Timoshenko and J.N. Goodier, *Theory of Elasticity* (third edition), McGraw-Hill Book Company, New York, N.Y. (1970).
13. R.W. Little, *Elasticity*, Prentice-Hall Incorporated, Englewood Cliffs, New Jersey (1973).

Appendix

Herein we furnish details of the auxiliary fields needed for the construction of eigenfunctions for the epoxy-steel butt joint. The first of these stress and displacement fields follow from differentiation of (15) and (16), respectively, once with respect to λ .

This gives, for the stresses,

$$\begin{aligned}\sigma_r = & -r^{\lambda-1} \{ \lambda \ln r [(\lambda-3)(\bar{a} \cos(\lambda-1)\theta + \bar{b} \sin(\lambda-1)\theta + \bar{c} \cos(\lambda+1)\theta + \bar{d} \sin(\lambda+1)\theta) \\ & + \lambda \theta [(\lambda-3)(-\bar{a} \sin(\lambda-1)\theta + \bar{b} \cos(\lambda-1)\theta - \bar{c} \sin(\lambda+1)\theta + \bar{d} \cos(\lambda+1)\theta) \\ & + (2\lambda-3)(\bar{a} \cos(\lambda-1)\theta + \bar{b} \sin(\lambda-1)\theta + \bar{c} \cos(\lambda+1)\theta + \bar{d} \sin(\lambda+1)\theta)],\end{aligned}$$

$$\begin{aligned}\sigma_\theta = & r^{\lambda-1} \{ \lambda \ln r [(\lambda+1)(\bar{a} \cos(\lambda-1)\theta + \bar{b} \sin(\lambda-1)\theta + \bar{c} \cos(\lambda+1)\theta + \bar{d} \sin(\lambda+1)\theta) \\ & + \lambda \theta [(\lambda+1)(-\bar{a} \sin(\lambda-1)\theta + \bar{b} \cos(\lambda-1)\theta - \bar{c} \sin(\lambda+1)\theta + \bar{d} \cos(\lambda+1)\theta) \\ & + (2\lambda+1)(\bar{a} \cos(\lambda-1)\theta + \bar{b} \sin(\lambda-1)\theta + \bar{c} \cos(\lambda+1)\theta + \bar{d} \sin(\lambda+1)\theta)],\end{aligned}$$

$$\begin{aligned}\tau_{r\theta} = & r^{\lambda-1} \{ \lambda \ln r [(\lambda-1)(\bar{a} \sin(\lambda-1)\theta - \bar{b} \cos(\lambda-1)\theta + \bar{c} \sin(\lambda+1)\theta - \bar{d} \cos(\lambda+1)\theta) \\ & + \lambda \theta [(\lambda-1)(\bar{a} \cos(\lambda-1)\theta + \bar{b} \sin(\lambda-1)\theta + \bar{c} \cos(\lambda+1)\theta + \bar{d} \sin(\lambda+1)\theta) \\ & + (2\lambda-1)(\bar{a} \sin(\lambda-1)\theta - \bar{b} \cos(\lambda-1)\theta + \bar{c} \sin(\lambda+1)\theta - \bar{d} \cos(\lambda+1)\theta)],\end{aligned}$$

in which $\bar{a}, \bar{b}, \bar{c}, \bar{d}$ are constants, the bar atop them serving to denote that they need not be the same as their antecedents, a, b, c, d . The corresponding displacements are

$$\begin{aligned}u_r = & \frac{-r^\lambda}{2\mu} \{ \ln r [(\lambda-\kappa)(\bar{a} \cos(\lambda-1)\theta + \bar{b} \sin(\lambda-1)\theta + \bar{c} \cos(\lambda+1)\theta + \bar{d} \sin(\lambda+1)\theta) \\ & + \theta [(\lambda-\kappa)(-\bar{a} \sin(\lambda-1)\theta + \bar{b} \cos(\lambda-1)\theta - \bar{c} \sin(\lambda+1)\theta + \bar{d} \cos(\lambda+1)\theta) \\ & + \bar{a} \cos(\lambda-1)\theta + \bar{b} \sin(\lambda-1)\theta],\end{aligned}$$

$$\begin{aligned}
u_{\theta} = \frac{r^{\lambda}}{2\mu} \{ & \ln r [(\lambda + \kappa)(\bar{a} \sin(\lambda - 1)\theta - \bar{b} \cos(\lambda - 1)\theta) + \bar{c} \sin(\lambda + 1)\theta - \bar{d} \cos(\lambda + 1)\theta] \\
& + \theta [(\lambda + \kappa)(\bar{a} \cos(\lambda - 1)\theta + \bar{b} \sin(\lambda - 1)\theta) + \bar{c} \cos(\lambda + 1)\theta + \bar{d} \sin(\lambda + 1)\theta] \\
& + \bar{a} \sin(\lambda - 1)\theta - \bar{b} \cos(\lambda - 1)\theta \}.
\end{aligned}$$

That these fields in fact satisfy the governing equations, (7), (8), may be verified by direct substitution. Satisfaction of these field equations, however, has to be the case since (15), (16) comply with (7), (8) for all λ , and (7), (8) do not themselves involve λ . It is of note that these fields contain terms that are distinct from the original ones in Williams [2], and which are not included in the classical solution of Michell (see e.g. Timoshenko and Goodier [12], p. 133, or even the extended version of Michell's solution given in Little [13], on pp. 166, 167).

Further differentiation gives the following stresses

$$\begin{aligned}
\sigma_r = -r^{\lambda-1} \{ & \lambda (\ln r)^2 [(\lambda - 3)(\hat{a} \cos(\lambda - 1)\theta + \hat{b} \sin(\lambda - 1)\theta) + \hat{c} \cos(\lambda + 1)\theta + \hat{d} \sin(\lambda + 1)\theta] \\
& + 2\lambda \theta \ln r [(\lambda - 3)(-\hat{a} \sin(\lambda - 1)\theta + \hat{b} \cos(\lambda - 1)\theta) - \hat{c} \sin(\lambda + 1)\theta + \hat{d} \cos(\lambda + 1)\theta] \\
& + 2 \ln r [(2\lambda - 3)(\hat{a} \cos(\lambda - 1)\theta + \hat{b} \sin(\lambda - 1)\theta) + \hat{c} \cos(\lambda + 1)\theta + \hat{d} \sin(\lambda + 1)\theta] \\
& + 2\theta [(2\lambda - 3)(-\hat{a} \sin(\lambda - 1)\theta + \hat{b} \cos(\lambda - 1)\theta) - \hat{c} \sin(\lambda + 1)\theta + \hat{d} \cos(\lambda + 1)\theta] \\
& - \lambda \theta^2 [(\lambda - 3)(\hat{a} \cos(\lambda - 1)\theta + \hat{b} \sin(\lambda - 1)\theta) + \hat{c} \cos(\lambda + 1)\theta + \hat{d} \sin(\lambda + 1)\theta] \\
& + 2(\hat{a} \cos(\lambda - 1)\theta + \hat{b} \sin(\lambda - 1)\theta) \},
\end{aligned}$$

$$\begin{aligned}
\sigma_{\theta} = r^{\lambda-1} \{ & \lambda (\ln r)^2 [(\lambda + 1)(\hat{a} \cos(\lambda - 1)\theta + \hat{b} \sin(\lambda - 1)\theta) + \hat{c} \cos(\lambda + 1)\theta + \hat{d} \sin(\lambda + 1)\theta] \\
& + 2\lambda \theta \ln r [(\lambda + 1)(-\hat{a} \sin(\lambda - 1)\theta + \hat{b} \cos(\lambda - 1)\theta) - \hat{c} \sin(\lambda + 1)\theta + \hat{d} \cos(\lambda + 1)\theta] \\
& + 2 \ln r [(2\lambda + 1)(\hat{a} \cos(\lambda - 1)\theta + \hat{b} \sin(\lambda - 1)\theta) + \hat{c} \cos(\lambda + 1)\theta + \hat{d} \sin(\lambda + 1)\theta] \\
& + 2\theta [(2\lambda + 1)(-\hat{a} \sin(\lambda - 1)\theta + \hat{b} \cos(\lambda - 1)\theta) - \hat{c} \sin(\lambda + 1)\theta + \hat{d} \cos(\lambda + 1)\theta] \\
& - \lambda \theta^2 [(\lambda + 1)(\hat{a} \cos(\lambda - 1)\theta + \hat{b} \sin(\lambda - 1)\theta) + \hat{c} \cos(\lambda + 1)\theta + \hat{d} \sin(\lambda + 1)\theta] \\
& + 2(\hat{a} \cos(\lambda - 1)\theta + \hat{b} \sin(\lambda - 1)\theta) \},
\end{aligned}$$

$$\begin{aligned}
\tau_{r\theta} = r^{\lambda-1} \{ & \lambda(\ln r)^2 [(\lambda-1)(\hat{a} \sin(\lambda-1)\theta - \hat{b} \cos(\lambda-1)\theta) + \hat{c} \sin(\lambda+1)\theta - \hat{d} \cos(\lambda+1)\theta] \\
& + 2\lambda \ln r [(\lambda-1)(\hat{a} \cos(\lambda-1)\theta + \hat{b} \sin(\lambda-1)\theta) + \hat{c} \cos(\lambda+1)\theta + \hat{d} \sin(\lambda+1)\theta] \\
& + 2 \ln r [(2\lambda-1)(\hat{a} \sin(\lambda-1)\theta - \hat{b} \cos(\lambda-1)\theta) + \hat{c} \sin(\lambda+1)\theta - \hat{d} \cos(\lambda+1)\theta] \\
& + 2\theta [(2\lambda-1)(\hat{a} \cos(\lambda-1)\theta + \hat{b} \sin(\lambda-1)\theta) + \hat{c} \cos(\lambda+1)\theta + \hat{d} \sin(\lambda+1)\theta] \\
& - \lambda\theta^2 [(\lambda-1)(\hat{a} \sin(\lambda-1)\theta - \hat{b} \cos(\lambda-1)\theta) + \hat{c} \sin(\lambda+1)\theta - \hat{d} \cos(\lambda+1)\theta] \\
& + 2(\hat{a} \sin(\lambda-1)\theta - \hat{b} \cos(\lambda-1)\theta) \},
\end{aligned}$$

in which $\hat{a}, \hat{b}, \hat{c}, \hat{d}$ are also independent constants. The associated displacements are

$$\begin{aligned}
u_r = \frac{-r^\lambda}{2\mu} \{ & (\ln r)^2 [(\lambda-\kappa)(\hat{a} \cos(\lambda-1)\theta + \hat{b} \sin(\lambda-1)\theta) + \hat{c} \cos(\lambda+1)\theta + \hat{d} \sin(\lambda+1)\theta] \\
& + 2\theta \ln r [(\lambda-\kappa)(-\hat{a} \sin(\lambda-1)\theta + \hat{b} \cos(\lambda-1)\theta) - \hat{c} \sin(\lambda+1)\theta + \hat{d} \cos(\lambda+1)\theta] \\
& + 2 \ln r [\hat{a} \cos(\lambda-1)\theta + \hat{b} \sin(\lambda-1)\theta] + 2\theta [-\hat{a} \sin(\lambda-1)\theta + \hat{b} \cos(\lambda-1)\theta] \\
& - \theta^2 [(\lambda-\kappa)(\hat{a} \cos(\lambda-1)\theta + \hat{b} \sin(\lambda-1)\theta) + \hat{c} \cos(\lambda+1)\theta + \hat{d} \sin(\lambda+1)\theta] \},
\end{aligned}$$

$$\begin{aligned}
u_\theta = \frac{r^\lambda}{2\mu} \{ & (\ln r)^2 [(\lambda+\kappa)(\hat{a} \sin(\lambda-1)\theta - \hat{b} \cos(\lambda-1)\theta) + \hat{c} \sin(\lambda+1)\theta - \hat{d} \cos(\lambda+1)\theta] \\
& + 2\theta \ln r [(\lambda+\kappa)(\hat{a} \cos(\lambda-1)\theta + \hat{b} \sin(\lambda-1)\theta) + \hat{c} \cos(\lambda+1)\theta + \hat{d} \sin(\lambda+1)\theta] \\
& + 2 \ln r [\hat{a} \sin(\lambda-1)\theta - \hat{b} \cos(\lambda-1)\theta] + 2\theta [\hat{a} \cos(\lambda-1)\theta + \hat{b} \sin(\lambda-1)\theta] \\
& - \theta^2 [(\lambda+\kappa)(\hat{a} \sin(\lambda-1)\theta - \hat{b} \cos(\lambda-1)\theta) + \hat{c} \sin(\lambda+1)\theta - \hat{d} \cos(\lambda+1)\theta] \}.
\end{aligned}$$

Again these fields may be verified by direct substitution in (7), (8). The foregoing auxiliary fields suffice for the construction of the eigenfunctions up to the terms explicitly given in Section 4; higher order terms require further auxiliary fields which can be generated by yet further differentiation.